Cancer Letters 443 (2019) 145–156

Contents lists available at ScienceDirect

Cancer Letters

journal homepage: www.elsevier.com/locate/canlet

Original Articles

MicroRNA-146b-5p as an oncomiR promotes papillary thyroid carcinoma development by targeting CCDC6

Meng Jia[a,b], Yang Shi[a], Zhuyao Li[a], Xiubo Lu[a,b,*], Jiaxiang Wang[a,b,**]

[a] The First Affiliated Hospital of Zhengzhou University, Zhengzhou, Henan, 450052, China
[b] Faculty of Medicine, Zhengzhou University, Zhengzhou, Henan, 450001, China

ARTICLE INFO

Keywords:
Papillary thyroid carcinoma
CCDC6
microRNA-146b-5p

ABSTRACT

The microRNA-146b–5p (miR-146b-5p) is known to be involved in the development of papillary thyroid cancer (PTC); however, the underlying mechanism is unclear. Here we have investigated the biological functions and underlying molecular mechanisms of miR-146b-5p in PTC. The expression of miR-146b–5p was assessed in 92 pairs of PTC and adjacent normal tissues and showed correlation with the clinicopathological status such as the tumour size. Effects of miR-146b-5p and its direct target, coiled-coil domain containing 6 (CCDC6), on cell proliferation, migration, invasion, and cell cycle were evaluated through gain- and loss-of-function studies *in vitro* and *in vivo*. The expression of CCDC6 was further examined in 187 PTC cases and was found to be correlated with the clinicopathological status. Overexpression of miR-146b-5p was observed in PTC tissues that correlated with advanced PTC. miR-146b-5p promoted cell proliferation, migration, invasion, and cell cycle progression *in vitro*, whereas CCDC6 reversed this effect. miR-146b-5p promoted PTC growth in a subcutaneous mouse model *in vivo*, whereas overexpression of CCDC6 exerted the opposite effect. In conclusion, miR-146b-5p expression correlated with advanced PTC and promoted PTC development by targeting CCDC6 *in vitro* and *in vivo*; it could, therefore, serve as a promising target for PTC treatment.

1. Introduction

The past three decades have witnessed growing incidences of thyroid cancer, which accounts for the majority of malignancies of the endocrine system [1]. Papillary thyroid carcinoma (PTC) constitutes about 80–85% of thyroid cancers [2]. The conventional management strategies, including thyroidectomy, radioiodine ablation, and adjuvant long-term thyrotropin suppression therapy, provide favourable treatment outcomes in the majority of PTC cases. However, the lack of treatment options for the individuals prone to recurrence and metastasis has stagnated the survival rate. Therefore, the understanding of the molecular mechanism of PTC development and metastasis is desirable for the development of novel targeted therapies [3,4].

MicroRNAs (miRNAs) are highly conserved, small non-coding RNAs that participate in carcinogenesis processes by base-pairing with the 3′-untranslated regions (UTRs) of target mRNAs at the post-transcriptional level [5,6]. Recent studies have indicated the formation and progression of PTC characterised with the aberrant expression of miRNAs, thereby presenting diagnostic and prognostic values [7–9]. We have previously demonstrated the remarkable upregulation in miR-146b-5p expression in PTC tissues as compared with the corresponding normal thyroid tissues [10]; however the molecular mechanism underlying miR-146b-5p-mediated aggravation of the malignant phenotypes of PTC cells is still unclear.

Coiled-coil domain-containing 6 (CCDC6), a ubiquitously expressed 65 kDa nuclear and cytosolic protein, was originally recognised as a product of chimeric genes caused by chromosomal translocation involving the RET proto-oncogene in approximately 20% of PTC and ~5% of lung adenocarcinoma [11–13]. Merolla et al. [14] showed that CCDC6 may act as a substrate of ataxia telangiectasia-mutated (ATM) gene and mediate the cellular response to DNA damage, while CCDC6 deficiency was associated with thyroid tumorigenesis. With a knock-in mouse model, Leone et al. [15] verified that CCDC6 contributed to PTC development by enhancing the activity of cAMP-response element-binding protein 1 (CREB1). We hypothesise that CCDC6 is a direct target of miR-146b-5p and may serve as a tumour suppressor involved in multiple biological processes such as viability, motility, and adhesion in PTC and that miR-146b-5p contributed to the malignant phenotype in PTC via suppression of CCDC6 expression.

In this study, we examined the expression and functional role of miR-146b-5p in PTC and its correlation with lymph node metastasis,

* Corresponding author. The First Affiliated Hospital of Zhengzhou University, Zhengzhou, Henan, 450052, China
** Corresponding author. The First Affiliated Hospital of Zhengzhou University, Zhengzhou, Henan, 450052, China
E-mail addresses: fccluxb@zzu.edu.cn (X. Lu), wjiaxiang@zzu.edu.cn (J. Wang).

https://doi.org/10.1016/j.canlet.2018.11.026
Received 30 September 2018; Received in revised form 21 November 2018; Accepted 24 November 2018

extra-thyroidal invasion, and advanced clinical TNM stages. We identified that CCDC6 was a direct target of miR-146b-5p in PTC and revealed that CCDC6-mediated miR-146b-5p expression promoted PTC development *in vitro* and *in vivo*. In addition, we examined the expression of CCDC6 in PTC tissues and found a negative correlation between CCDC6 expression and cervical lymph node metastasis, extra-thyroidal invasion, and advanced clinical TNM stages.

2. Materials and methods

2.1. Ethics approval

The collection and application of patient specimens involved in all experimental protocols were approved by the Human Ethics Committee of The First Affiliated Hospital of Zhengzhou University. Written informed consent was obtained from the patients. All animal research protocols were conducted in accordance with national and international guidelines and approved by the Animal Care and Use Institutional Review Board of The First Affiliated Hospital of Zhengzhou University.

2.2. Clinical specimens

A cohort containing 92 snap-frozen primary PTC and adjacent non-cancerous tissues (for miR-146b-5p study), and another cohort containing 187 formalin-fixed paraffin-embedded (FFPE) PTC and adjacent non-cancerous tissues (for CCDC6 study), were obtained from patients who underwent thyroidectomy from March 2015 to November 2015 at The First Affiliated Hospital of Zhengzhou University (Zhengzhou, Henan, China). All specimens were diagnosed and classified according to the TNM [16] staging system by two independent pathologists. The detailed clinical characteristics of samples from the two cohorts are presented in Tables 1 and 2.

2.3. Cell lines and cell culture

TPC-1, BCPAP, and Nthy-ori 3–1 (NTHY) cell lines were cultured in RPMI-1640 medium (Corning, NY, USA) supplemented with 10% foetal bovine serum (FBS; Gibco, Grand Island, NY, USA). All cells were cultured in a humidified atmosphere of 5% CO_2 at 37 °C.

Table 1
Clinicopathological characteristics of the 92 PTC patients for miR-146b-5p study.

Parameters	miRNA levels (miR-146b-5p/U6)		N	p-value
	Low (0–2)	High (3–4)		
Tissue Type				
PTC	40	52	92	*** < 0.001
Adjacent Normal	92	0	92	
Age				
< 45	16	24	40	0.642
≥45	24	28	52	
Gender				
Male	14	22	36	0.587
Female	26	30	56	
Tumour size				
≤2 cm	22	30	52	0.393
> 2 cm, ≤4 cm	15	17	32	
> 4 cm	3	5	8	
Lymph node metastasis				
Yes	12	29	41	*0.0446
No	28	23	51	
Extra-thyroidal invasion				
Yes	2	19	21	**0.0011
No	38	33	71	
TNM				
I	28	20	48	*** < 0.001
II	6	9	15	
III/IV	6	23	29	

PTC, papillary thyroid carcinoma; *p < 0.05; **p < 0.01; ***p < 0.001.

Table 2
Clinicopathological characteristics of the 187 PTC patients for CCDC6 study.

Parameters	CCDC6 levels(IHC scores)				N	p-value
	0	1	2	3 or 4		
Tissue type						
PTC	127	39	18	3	187	*** < 0.001
Adjacent Normal	19	27	43	98	187	
Age						
< 45	59	18	7	1	85	0.613
≥45	68	21	11	2	102	
Gender						
Male	57	18	7	0	82	0.539
Female	70	21	11	3	105	
Tumour size						
≤2 cm	81	26	8	0	115	0.308
> 2 cm, ≤4 cm	32	8	6	2	48	
> 4 cm	14	5	4	1	24	
Lymph node metastasis						
Yes	56	11	4	0	69	**0.009
No	71	28	14	3	118	
Extra-thyroidal invasion						
Yes	23	13	8	0	44	**0.003
No	110	18	12	3	143	
TNM						
I	71	18	10	2	101	*0.044
II	22	6	3	1	32	
III/IV	47	5	2	0	54	

PTC, papillary thyroid carcinoma; *p < 0.05; **p < 0.01; ***p < 0.001.

2.4. Extraction of RNA and quantitative real-time PCR (qRT-PCR) analysis

Total RNA was extracted using the Purelink™ RNA mini kit (Thermo Fisher Scientific, MA, USA) according to the manufacturer's instructions. For the quantitative analysis of mature miR-146b-5p, total RNA was reverse-transcribed into cDNA using the miRcute miRNA First-Strand cDNA Synthesis Kit (Tiangen Biotech, Beijing, China) and quantified through qRT-PCR using the miRcute miRNA qPCR Detection Kit SYBR Green (Tiangen Biotech, Beijing, China) according to the manufacturer's instructions.

For the detection of mRNAs, total RNA was reverse-transcribed using PrimeScript™ RT reagent Kit (TaKaRa, Dalian, China) prior to the amplification step to perform qRT-PCR using SYBR® Premix Ex Taq™ (TaKaRa, Dalian, China), according to the manufacturer's protocols. The relative expression of miRNAs and target mRNAs were normalised against U6 and glyceraldehyde 3-phosphate dehydrogenase (GAPDH), respectively, and analysed by the $2^{-\Delta\Delta CT}$ method. The sequences of the primers are listed in Supplementary Table 1.

2.5. Western blot analysis

Radioimmunoprecipitation assay (RIPA) lysis buffer (Cwbiotech, Beijing, China) supplemented with a protease inhibitor cocktail (Cwbiotech, Beijing, China) was used to extract proteins from the transfected cells. A bicinchoninic acid protein assay kit (Cwbiotech, Beijing, China) was used to quantify the concentration of total proteins. Proteins were subsequently separated on a 10% sodium dodecyl sulphate polyacrylamide gel electrophoresis (SDS-PAGE) gel and transferred onto polyvinylidene difluoride membranes (Roche Applied Science, IN, USA). The membranes were blocked with 5% skimmed milk (BD Biosciences, CA, USA) at room temperature for 2 h, prior to overnight incubation with primary antibodies at 4 °C. The membranes were subsequently incubated with secondary antibodies at room temperature for 2 h, followed by detection of protein bands using the Pierce ECL Western Blotting Substrate (Thermo Scientific, IL, USA). The antibodies used for western blot analysis were as follows: mouse anti-human CCDC6 primary antibody (1:250; Sigma-Aldrich, MO, USA), mouse anti-human β-actin primary antibody (as a loading control), and

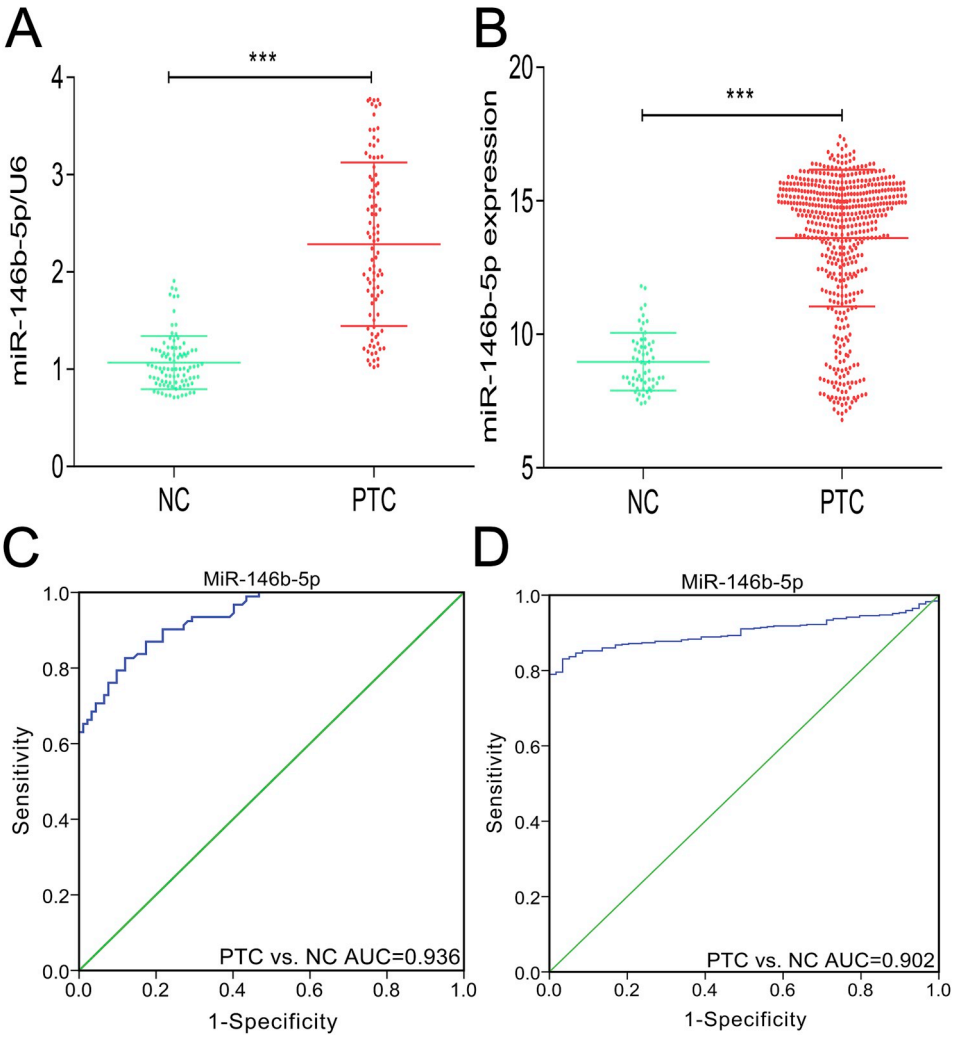

Fig. 1. miR-146b-5p expression is up-regulated in PTC. (A) Comparison of the expression level of miR-146b-5p in (A) papillary thyroid carcinoma tissues (PTC, n = 92) and the corresponding non-carcerous tissues (NC, n = 92). (B) Comparison of the expression level of miR-146b-5p in data from TCGA datasets (PTC, n = 512; NC, n = 59). Receiver operating characteristic (ROC) curve of miR-146b-5p for diagnostic value of PTCs from NCs in tissue specimen (C) and TCGA datasets (D). Data are represented as the mean ± SD of triplicate experiments. NS, non-significant; *p < 0.05; **, p < 0.01; and ***p < 0.001.

goat anti-mouse horseradish peroxidase conjugated secondary antibody (Cell Signalling Technology, MA, USA).

2.6. Synthesis of oligonucleotides and transient transfection

The miR-146b-5p mimic, miR-146b-5p inhibitor, siCCDC6, and their negative control (NC) RNAs were synthesised by Genepharma (Shanghai, China), and their sequences are listed in Supplementary Table 2. Transfection was performed with TPC-1 and BCPAP cells using Lipofectamine® 2000 (Invitrogen, Carlsbad, CA, USA), as per the manufacturer's instructions.

2.7. Plasmid and lentivirus constructions

For the construction of a lentiviral vector that stably expressed miR-146b-5p inhibitor, an oligonucleotide strand with a complementary miR-146b-5p mature sequence (http://www.miRbase.org) was cloned between *Age*I and *Eco*RI sites of pGV280-hU6-MCS-EGFP-puromycin (GeneChem, Shanghai, China). For the construction of the lentiviral vector stably expressing CCDC6, the coding sequence of CCDC6 (NM_005436.4) was inserted between *Age*I and *Nhe*I sites of pGV367-Ubi-MCS-EGFP-puromycin (GeneChem, Shanghai, China). Cells were transfected with the packaged lentivirus and selected with puromycin (2 μg/mL; Sigma-Aldrich, Co. LLC, MO, USA). The wild-type (WT) 3′-UTR of CCDC6 amplified by the primers containing the putative seed region sequences of miR-146b-5p-binding sites was inserted downstream of the firefly luciferase gene between *Sac*I and *Xho*I sites of the pmirGLO vector (Biofeng Inc., Shanghai, China). Site-directed mutagenesis of the miR-146b-5p-binding site in CCDC6 3′-UTR was performed using the NEB Q5® Site-Directed Mutagenesis Kit (New England Biolabs Inc., MA, USA). The recombinant plasmids were purified using the High Pure Maxi Plasmid Kit (Tiangen Biotech, Beijing, China). All primers and sequence involved in this section are listed in Supplementary Table 3.

2.8. Cell proliferation assay

Cell counting kit-8 (CCK-8; Dojindo Laboratories, Kumamoto, Japan) was used to determine the viability of TPC-1 and BCPAP cells after transfection with miR-146b-5p mimic and miR-NC mimic. Cells were inoculated into 96-well plates (Corning, NY, USA) at a density of 4×10^3 cells/well and incubated for 24, 48, 72, and 96 h. CCK-8 reagent (10 μL) was added to each well and the plate was incubated for 2 h, followed by the measurement of absorbance at 450 nm with a spectrophotometer (Bio-Rad, CA, USA).

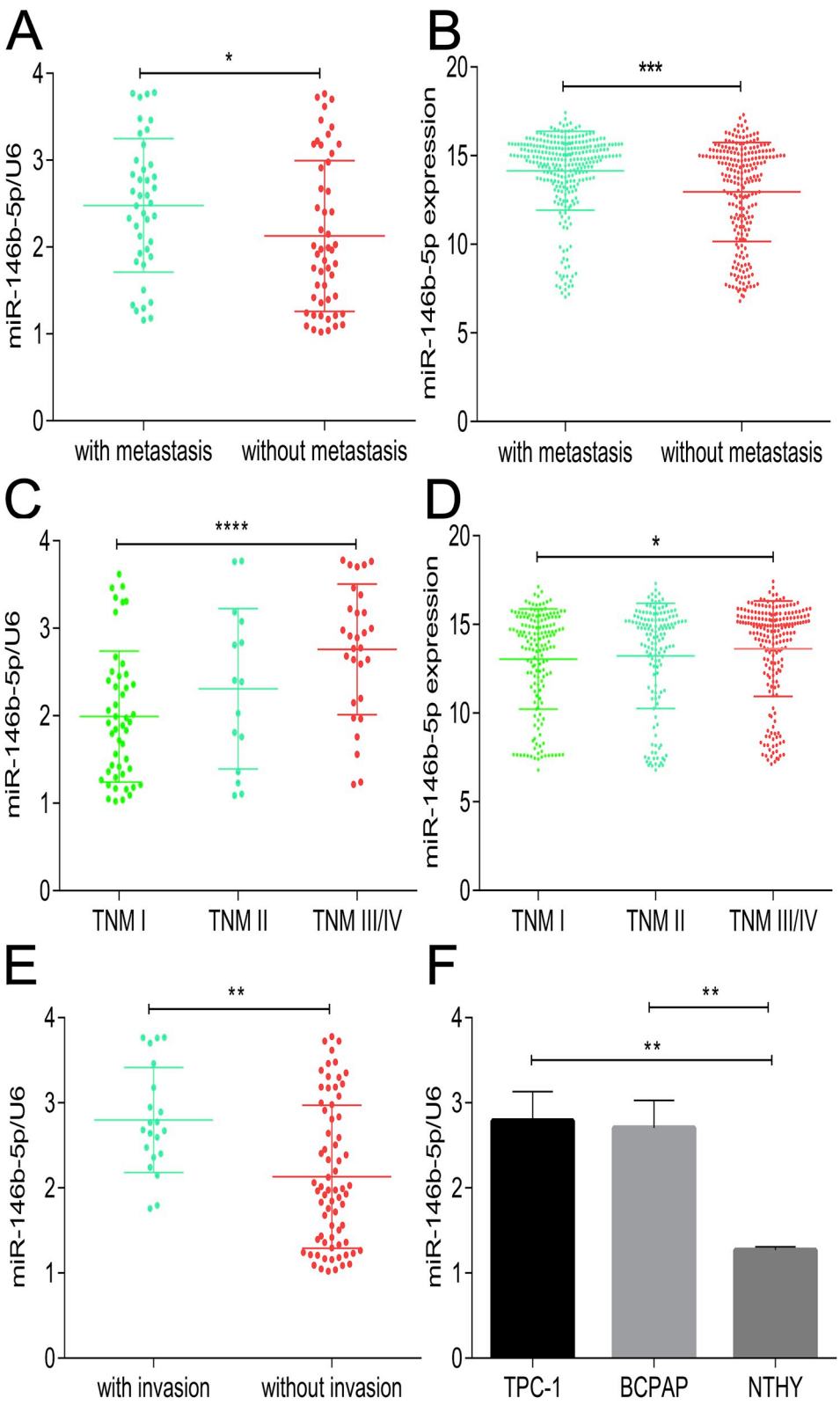

Fig. 2. miR-146b-5p expression is significantly associated with advanced stages or metastasis of PTC. Expression of miR-146b-5p in PTC tissues with (n = 41) or without (n = 51) lymph node metastasis (A) and data from TCGA dataset (with, n = 282; without, n = 230) (B). Expression of miR-146b-5p in PTC tissues at different clinical TNM stages (TNM I, n = 48; TNM II, n = 15; TNM III/IV, n = 29) (C) and data from TCGA dataset (TNM I, n = 162; TNM II, n = 142; TNM III/IV, n = 208) (D). (E) Expression of miR-146b-5p in PTC tissues with (n = 21) or without (n = 71) extra-thyroidal invasion. (F) Endogenous expression levels of miR-146b-5p in TPC-1, BCPAP, and NTHY cell lines. Data are represented as the mean ± SD of triplicate experiments. *p < 0.05, **p < 0.01, ***p < 0.001, and ****p < 0.0001.

2.9. Wound-healing assay

For the wound-healing assay, cells were seeded into six-well plates at a density of 2×10^6 cells/well. The monolayer was scratched with a 20-μL pipette tip and the cells were cultured with fresh medium without FBS. The closure of the wound was observed and photographed under an inverted microscope (Leica, Germany) at different time points (0, 24, and 36 h).

2.10. Invasion assay

Transwell® chambers (bore diameter of 8 μm; Corning, NY, USA) in a 24-well plate were used to evaluate the invasive ability of different cells. Briefly, 1×10^5 cells from each experimental group resuspended in 200 μL of RPMI-1640 medium without FBS were seeded into the upper insert, while the lower insert was filled with 600 μL of fresh

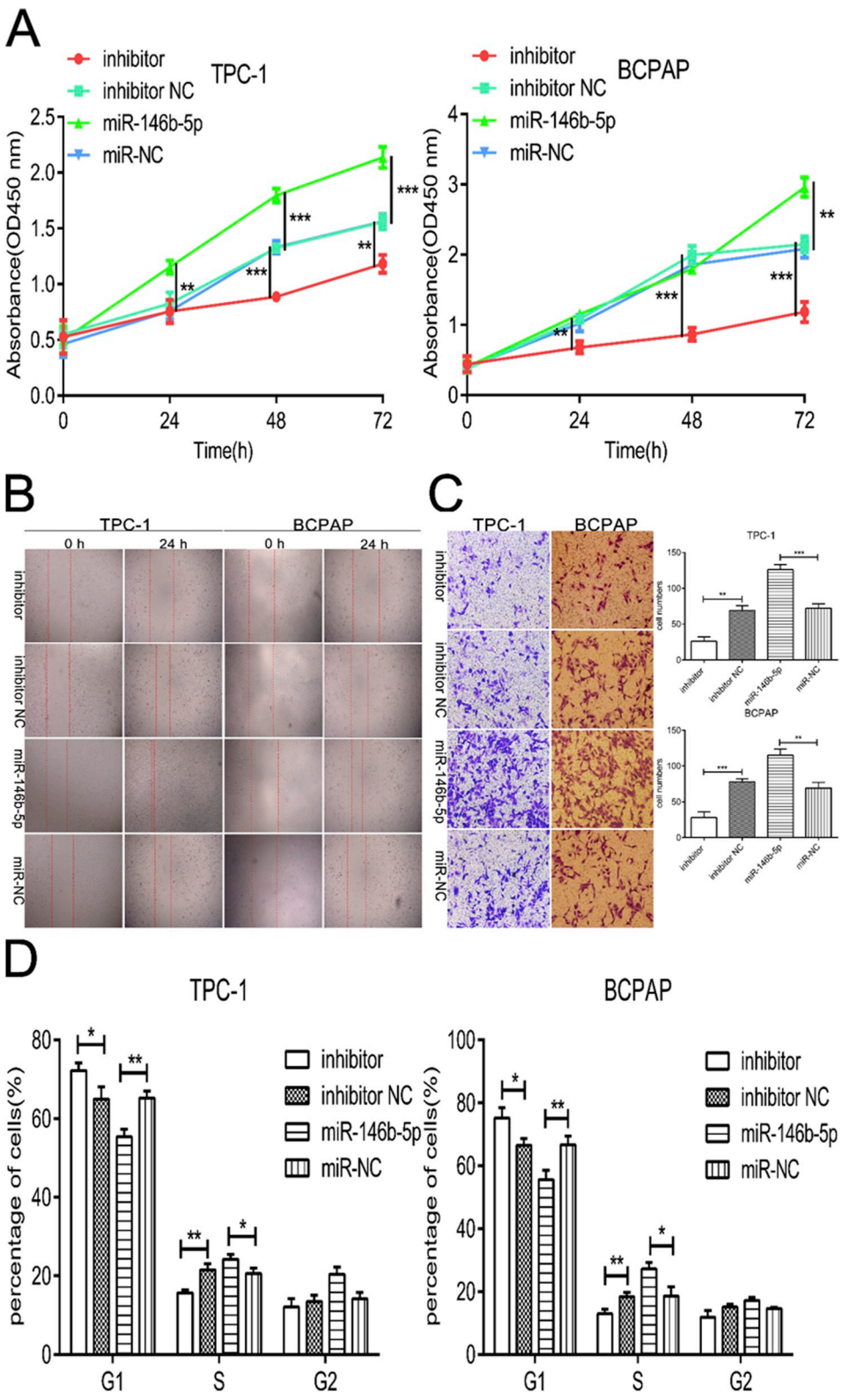

Fig. 3. miR-146b-5p is functionally involved in the biological behaviours of PTC *in vitro*. (A) Overexpression of miR-146b-5p promotes cell proliferation while silencing of miR-146b-5p inhibits cell proliferation in both TPC-1 and BCPAP PTC cell lines. (B) Overexpression of miR-146b-5p promotes cell migration while silencing of miR-146b-5p inhibits cell migration using wound-healing assays in both TPC-1 and BCPAP PTC cell lines. (C) Overexpression of miR-146b-5p promotes cell invasion while silencing of miR-146b-5p inhibits invasion in both TPC-1 and BCPAP PTC cell lines. (D) Flow cytometry analysis revealed that miR-146b-5p accelerated cell cycle progression (G0/G1 to S phase) in both TPC-1 and BCPAP PTC cells.

complete medium. After a 24 h incubation at 37 °C and 5% CO_2, the cells that had invaded to the lower surface of the gel were fixed in 4% paraformaldehyde and stained with 0.1% crystal violet. The average number of the invaded cells was calculated in five random fields (200 ×) per insert.

2.11. Cell cycle and apoptosis analysis

For cell cycle analysis, cells were harvested and resuspended in phosphate-buffered saline (PBS) at a density of 1×10^6 cells/mL after 48 h of transfection, followed by an overnight treatment with ice-cold

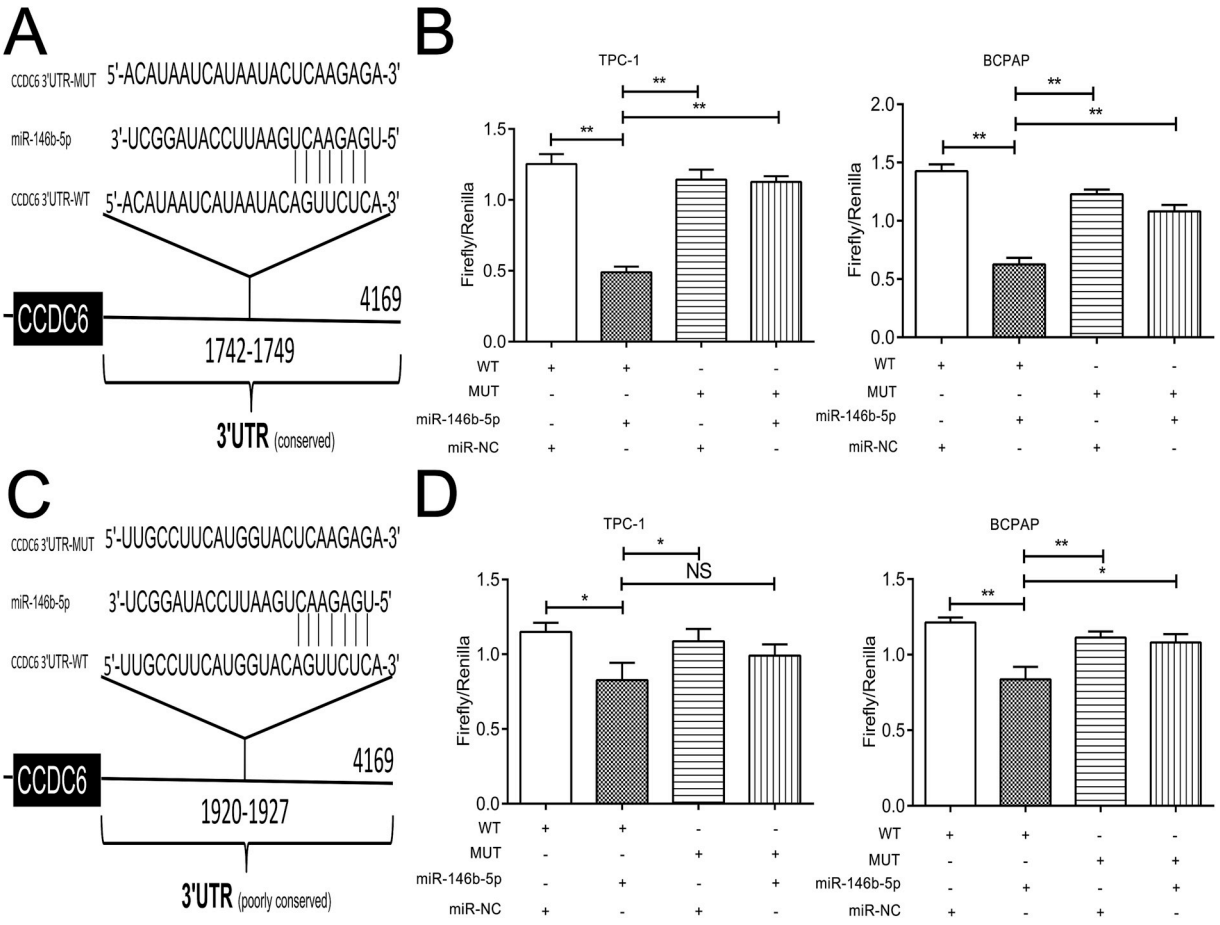

Fig. 4. MiR-146b-5p directly targets CCDC6 via its 3′- UTR. Sequence alignment of the miR-146b-5p base-paring sites in the predicted conserved (A) and poorly conserved (C) 3′-UTRs of CCDC. Co-transfection CCDC6 3′-UTR constructs [WT1 (conserved) and MUT1 (B), WT2 (poorly conserved) and MUT2 (D)] with miR-146b-5p in TPC-1and BCPAP cells. Luciferase activity is presented as the ratio of Firefly/Renilla luciferase activity. Data are represented as the mean ± SD of triplicate experiments. UTR, untranslated regions; NS, non-significant. *p < 0.05, **p < 0.001.

70% ethanol for fixation. According to the manufacturer's instructions of Cell Cycle Detection Kit (KeyGEN Co. Ltd., Nanjing, China), the suspension was incubated with 100 μL of RNase A for 30 min at 37 °C, followed by the treatment with propidium iodide (PI) for 30 min in the absence of light before flow cytometry analysis (MoFlo XDP flow cytometer; Beckman Coulter, MA, USA).

For apoptosis analysis, cells were harvested and resuspended in PBS at a density of 5×10^5 cells/mL after 48 h of transfection. According to the manufacturer's instructions of the Annexin V-APC/PI Apoptosis Detection Kit (KeyGEN Co. Ltd., Nanjing, China), cells were re-suspended in 300 μL of a binding buffer and stained with 5 μL of Annexin V/APC and 5 μL of PI. The stained cells were incubated at room temperature for 15 min in the absence of light prior to flow cytometry (MoFlo XDP flow cytometer, Beckman Coulter, MA, USA).

2.12. Dual-luciferase reporter assays

For dual-luciferase reporter assay analysis, co-transfection was performed with reporter construction (WT1 and MUT1, WT2 and MUT2) and the corresponding miR-146b-5p mimic or miR-NC mimic in TPC-1 and BCPAP cells with Lipofectamine 2000 (Invitrogen). After 48 h co-transfection, luciferase activity was recorded using Cetro XS3 LB 960 microplate luminometer (Berthold, Bad Wildbad, Germany) and normalised against the luciferase activity of *Renilla*.

2.13. Immunohistochemistry (IHC) assessment

For the evaluation of CCDC6 expression in 187 paraffin-embedded PTC sections and the corresponding normal sections, IHC was performed using the 3,3′-diaminobenzidine (DAB) Detection Kit (ZSGB-Bio Co. Ltd., Beijing, China). Briefly, sections (4 mm) were sequentially deparaffinized, re-hydrated, treated with 3% hydrogen peroxide (H_2O_2), and blocked with 5% goat serum. Samples were overnight incubated with an anti-CCDC6 antibody (1:200; Sigma-Aldrich, Co. LLC, MO, USA) at 4 °C, followed by treatment with an horseradish peroxidase-labelled secondary antibody (ZSGB-Bio Co. Ltd., Beijing, China) at room temperature for 1 h. Immunoreactivity was developed with DAB (ZSGB-Bio Co. Ltd., Beijing, China) containing 0.03% H_2O_2 and counterstained with haematoxylin and mounted. Negative controls were identically treated but using mouse IgG as the primary antibody.

Staining intensity of CCDC6 was independently scored by two experienced pathologists in five random fields (200 ×). The criteria used for assessment were as follows: score 0 for < 5% (positive cells), score 1 for 0–20%, score 2 for 20–50%, and score 3/4 for > 50%.

2.14. Mouse experiments

Sixteen female BALB/c-nude mice (4–6 weeks old; Vital River Inc., Beijing, China) were randomly allocated into four groups (n = 4 per

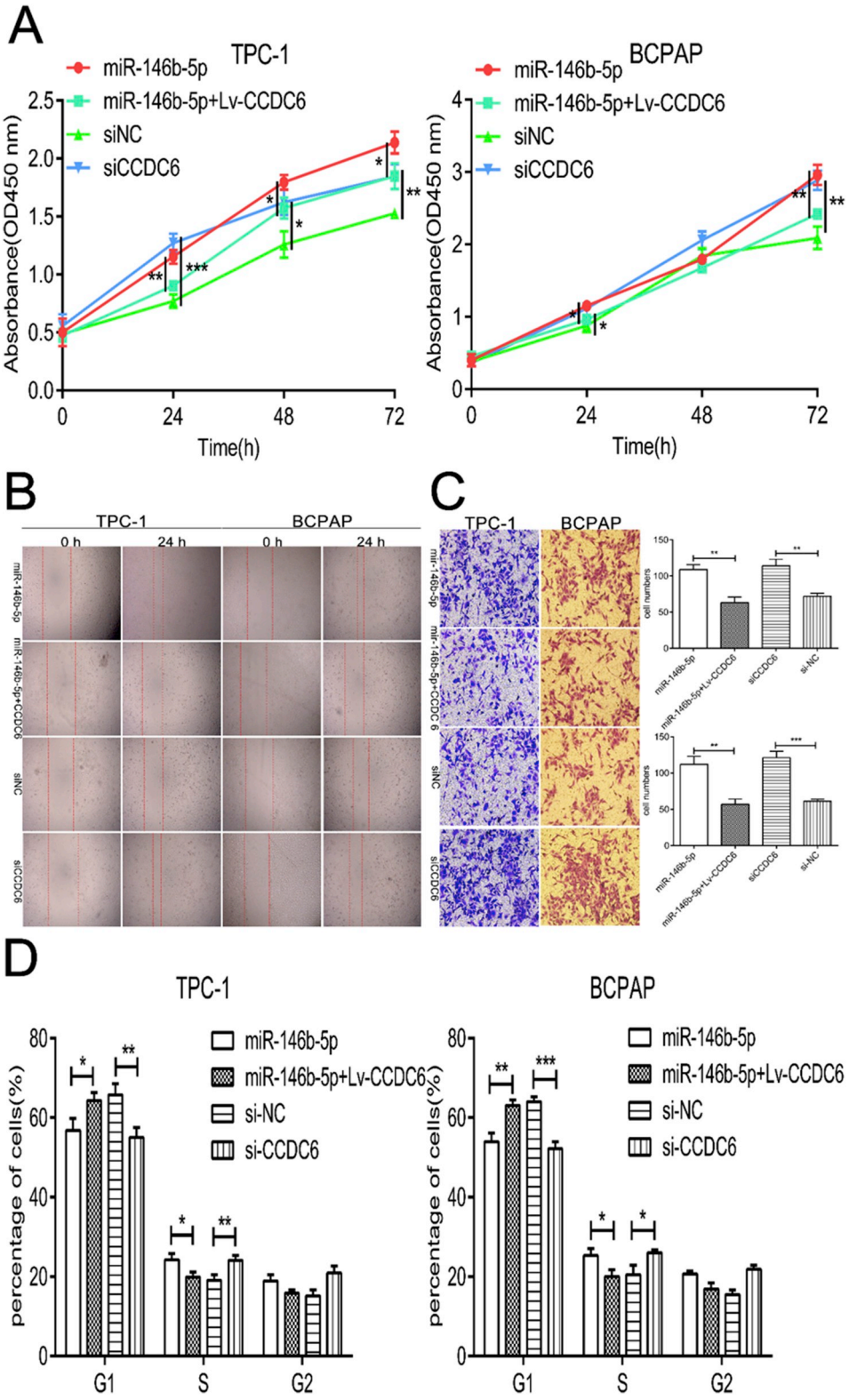

Fig. 5. Restoration of CCDC6 attenuates the promoting effects of miR-146b-5p on proliferation (A), migration (B), invasion (C), and cell cycle progression (D) in TPC-1 and BCPAP cells. Data are presented as mean ± SD of triplicate experiments. Lv-CCDC6, Lenti-pGV367-CCDC6; siCCDC6, CCDC6 siRNA; siNC, siRNA negative control. *p < 0.05, **p < 0.01.

group). TPC-1 cells that were transfected with Lenti-miR-146b-5p-inhibitor, Lenti-miR-NC, Lenti-pGV367-CCDC6, or Lenti-pGV367-NC were resuspended in PBS. An aliquot of 3.0×10^6 cells/100 μL of PBS was subcutaneously injected into the right flanks of mice. Tumour size was recorded every 7 days using a calliper, and volumes were calculated based on the following formula: Volume = $(L \times W^2)/2$, with L being the largest diameter (mm) and W being the smallest diameter (mm). The mice were sacrificed after 28 days and tumour weights were documented. Tumour tissues were reserved as appropriate for western blotting, qRT-PCR, and IHC.

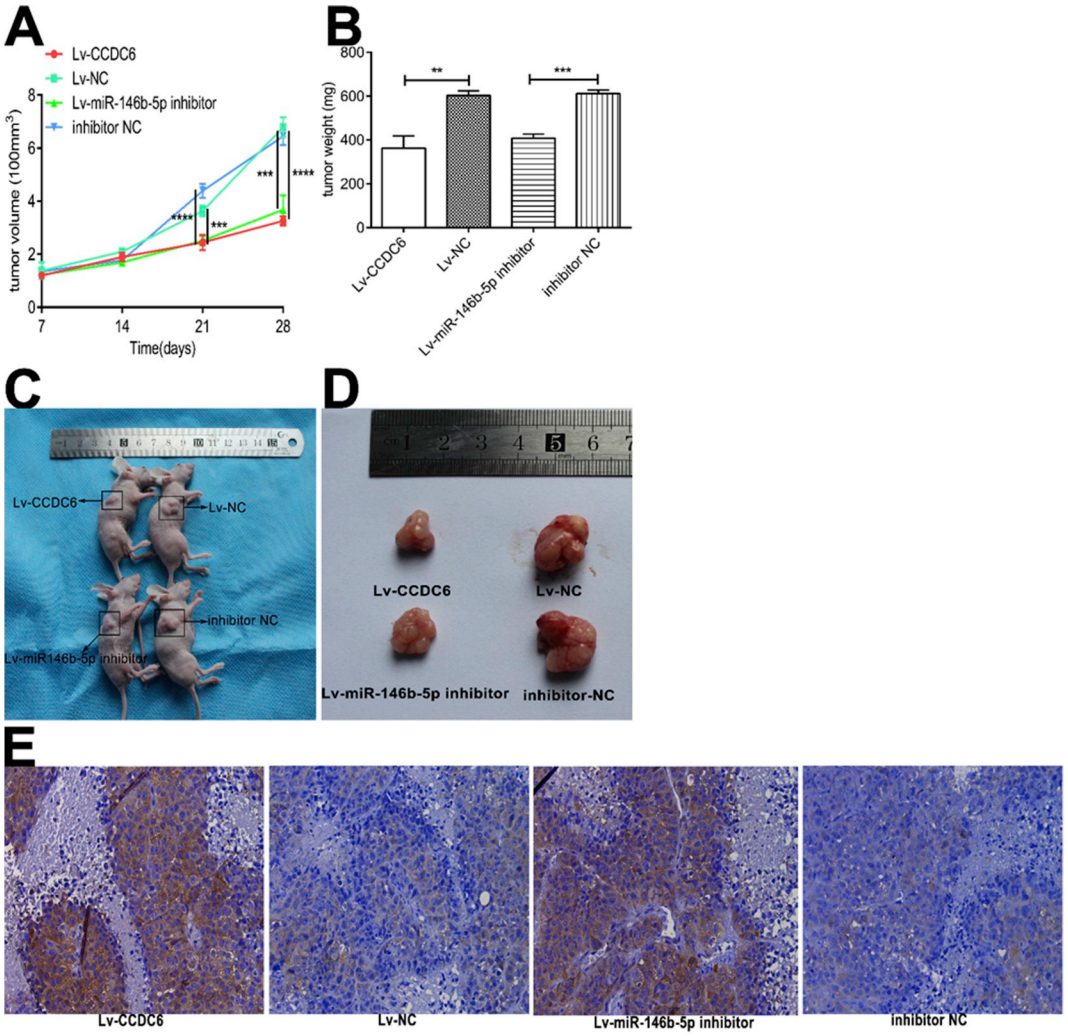

Fig. 6. Inhibition of miR-146b-5p or overexpression of CCDC6 suppresses TPC-1 cells proliferation *in vivo*. (A) Tumours derived from miR-146b-5p-silencing, CCDC6-overexpressing and control TPC-1 cells were harvested from the mice at 28 days post-inoculation. Tumour volumes were documented every week. (B) Tumour weights are significantly lower in miR-146b-5p-silencing and CCDC6-overexpressing, compared to their corresponding control group, respectively. Representative images of tumour-bearing nude mice and tumour xenografts were shown (C and D). (E) Immunohistochemistry analysis showed CCDC6 overexpression in CCDC6-overexpressing and miR-146b-5p-silencing xenograft FFPE sections, compared to their corresponding control group, respectively. The brown colour is positive staining. (Magnification 200 ×). Numerical data are represented as the mean ± SD of triplicate experiments. FFPE, formalin-fixed paraffin-embedded, Lv-CCDC6, Lenti-pGV367-CCDC6; Lv-NC, Lenti-pGV367 Negative Control; siCCDC6, CCDC6 siRNA; siNC, siRNA negative control. **p < 0.01, ***p < 0.01, ****p < 0.0001. (For interpretation of the references to color in this figure legend, the reader is referred to the Web version of this article.)

2.15. Statistical analysis

Statistical analyses were performed using SPSS version 21.0 software and GraphPad Prism version 6.0. Comparisons of quantitative variables and categorical variables among two groups were analysed by two-tailed Student's *t*-test and Chi-squared tests, respectively. Receiver operating characteristic (ROC) curves were established to evaluate the diagnostic value of miR-146b-5p. Multi-group polytomous ordinal response variable comparisons were performed by Kruskal-Wallis H test, and the correlation between the results was assessed with Spearman's test. Data were represented as the mean ± standard deviation (SD) of triplicate experiments. A value of $p < 0.05$ was considered statistically significant. NS = non-significant. *p < 0.05, **p < 0.01, and ***p < 0.001.

3. Results

3.1. Expression of miR-146b-5p is upregulated in PTC

We performed RT-qPCR analysis to investigate miR-146b-5p expression level in 92 snap-frozen primary PTC tissues and adjacent non-carcinomatous tissues. The characteristics of the participants are listed in Table 1 miR-146b-5p expression was distinctly increased in PTC tissues as compared to the corresponding non-cancerous tissues (Fig. 1A). In The Cancer Genome Atlas (TCGA) cohort, the expression level of miR-146b-5p was significantly higher in primary PTC tissues than in the control tissues (Fig. 1B).

3.2. MiR-146b-5p exhibits good diagnostic potential for PTC

We performed ROC curve analysis to assess the diagnostic value of miR-146b-5p for PTC. The comparison between PTC tissues and normal tissues revealed an area under the curve (AUC) of 0.936 (95% confidence interval [CI] = 0.904–0.967) for miR-146b-5p (Fig. 1C). Further comparison with TCGA cohort revealed an AUC value of 0.902 (95% CI = 0.877–0.926) for miR-146b-5p (Fig. 1D). These results indicate that miR-146b-5p may be used to differentiate between patients with PTC and controls and serve as a suitable biomarker for the diagnosis of PTC.

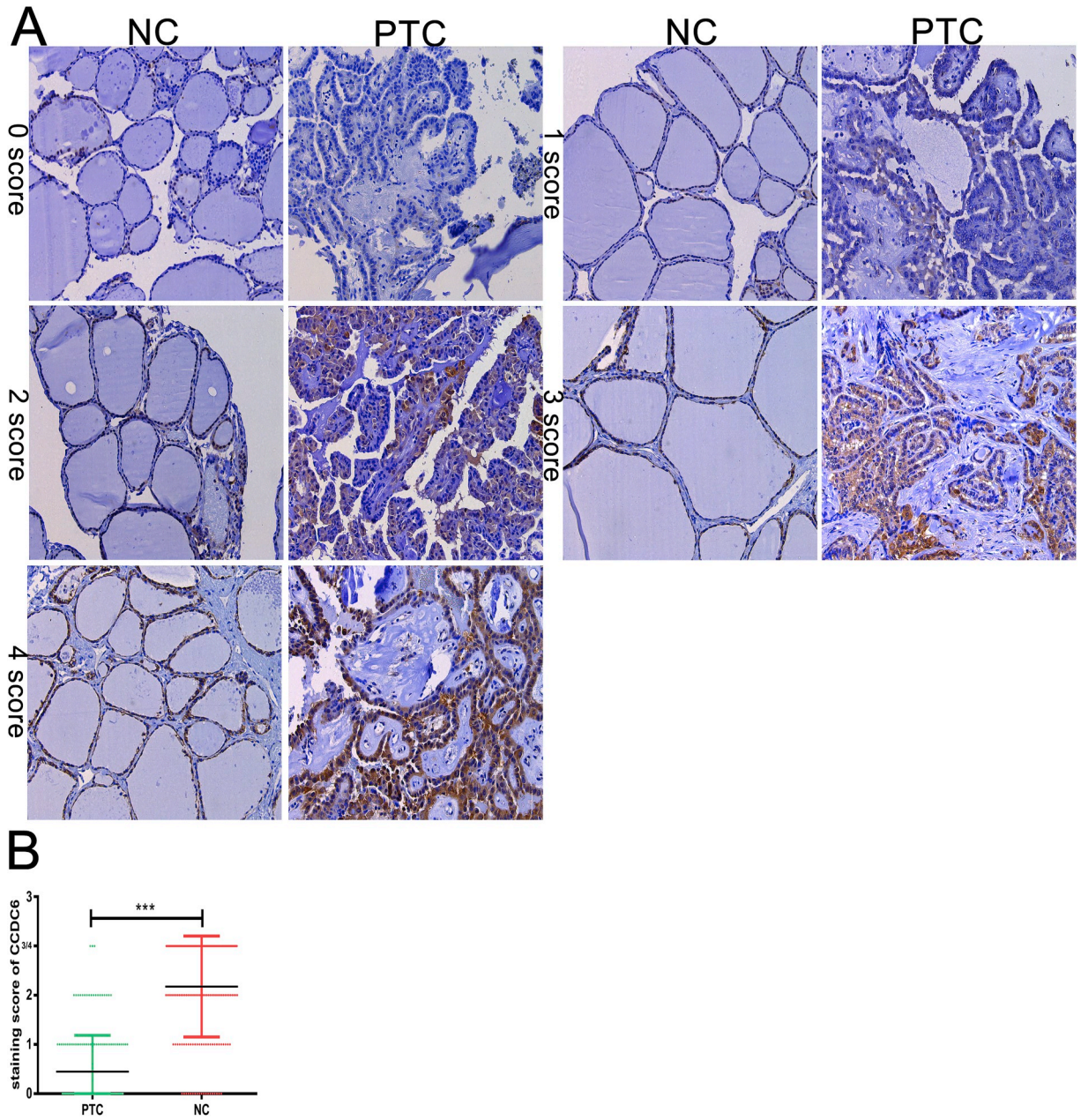

Fig. 7. CCDC6 expression in PTC and normal tissue sections and correlation. (A) Immunohistochemical staining for CCDC6 in PTC and normal FFPE sections (Magnification 200 ×). (B) The expression level of CCDC6 was significantly lower in PTC tissues compared with that in normal tissues. FFPE, formalin-fixed paraffin-embedded; NC, normal control; PTC, papillary thyroid carcinoma.

3.3. Overexpression of miR-146b-5p is associated with the malignant behaviour of PTC

The correlation between miR-146b-5p expression and clinicopathological status of PTC was assessed in tissues and TCGA cohorts. miR-146b-5p expression was higher in the PTC group with metastasis than in the PTC group without metastasis (Fig. 2A), consistent with the results for TCGA cohort (Fig. 2B). Furthermore, miR-146b-5p expression was higher in the advanced stages of PTC (III/IV) than in the early stages of PTC (I/II) (Fig. 2C), as observed with TCGA results (Fig. 2D). Moreover, the elevated expression level of miR-146b-5p was closely associated with extra-thyroidal invasion (Fig. 2E). An increase in the expression level of miR-146b-5p was observed in both TPC-1 and BCPAP PTC cell lines as compared to the human thyroid epithelial cell line NTHY (Fig. 2F). Overall, these results indicate that high level of miR-146b-5p expression was associated with clinically advanced stages of PTC and PTC metastasis.

3.4. miR-146b-5p promotes proliferation, migration, invasion, and cell cycle progression of PTC cells in vitro

To examine the biological functions of miR-146b-5p in PTC progression, gain- and loss-of-function studies were performed in TPC-1 and BCPAP cell lines following transfection with miR-146b-5p mimic, miR-NC mimic, miR-146b-5p inhibitor, and miR-inhibitor-NC.

The results of the CCK-8 proliferation assay showed that the upregulated expression of miR-146b-5p significantly increased the proliferation of cells as compared with the control group over a 72 h period in both cell lines, while miR-146b-5p downregulation significantly decreased the proliferation of these cell lines (Fig. 3A).

The results of the wound healing assay demonstrated that the inhibition of miR-146b-5p expression greatly impaired the closure of the wound in both cell lines. On the contrary, the overexpression of miR-146b-5p promoted the migratory ability in both cell lines (Fig. 3B).

As shown in Fig. 3C, the results from the Matrigel® transwell assay indicate that depletion of miR-146b-5p expression significantly reduced the invasiveness of TPC-1 and BCPAP cells, while the upregulation of miR-146b-5p expression improved the invasive ability of both cell types.

We used flow cytometric analysis to confirm that miR-146b-5p expression accelerates cell cycle progression (G0/G1 to S phase) in both cell types (Fig. 3D). Cell apoptosis was assessed using flow cytometry; however, no statistical difference was observed in response to the upregulated or downregulated expression of miR-146b-5p in both cell lines (data not shown).

Therefore, miR-146b-5p was closely related to the proliferative, migratory, and invasive abilities of, as well as cell cycle distribution in TPC-1 and BCPAP PTC cell lines. These findings suggest an oncogenic role of miR-146b-5p, as demonstrated by the malignant phenotypes of PTC cells, including proliferation, migration, invasion, and cell cycle progression *in vitro*.

3.5. miR-146b-5p downregulated CCDC6 expression by binding to its 3′-UTR

To understand the mechanism underlying the oncogenic effects of miR-146b-5p, we identified several putative target genes based on three publicly available miRNA databases (TargetScan, Diana, and miRanda). Bioinformatic analysis presented two speculative imperfect complementary sequences of miR-146b-5p, which exist in the 3′-UTR of CCDC6 mRNA (Fig. 4A and C). As shown in Fig. 4B and D, the mRNA and protein levels of CCDC6 significantly decreased in both the cell types transfected with miR-146b-5p mimic as compared with those transfected with miR-NC mimic. To confirm the direct inhibitory effect of miR-146b-5p on CCDC6 expression, a dual-luciferase reporter assay was performed. In comparison with the mutant-type luciferase report plasmid (MUT1-CCDC6-3′-UTR construct), the wild-type luciferase report plasmid (WT1-CCDC6-3′-UTR construct) lost the luciferase activity upon reintroduction of miR-146b-5p expression. The co-transfection with miR-NC mimic and the plasmids mentioned above in both cell types had no effect on the luciferase activity (Fig. 4B). The same results were demonstrated with WT2/MUT2-CCDC6-3′-UTR construct (Fig. 4D). Taken together, these results demonstrate that CCDC6 is a direct target of miR-146b-5p.

3.6. Restoration of CCDC6 expression mitigates miR-146b-5p-induced enhancement in proliferation, migration, invasion, and cell cycle progression in vitro

To investigate the functional relationship between CCDC6 and carcinogenetic effects of miR-146b-5p, TPC-1 and BCPAP cells were treated with miR-146b-5p mimic, miR-NC mimic, miR-146b-5p mimic plus Lenti-pGV367-CCDC6, CCDC6 siRNA, or siRNA-NC. The overexpression of CCDC6 resulted in the attenuation of miR-146b-5p-induced increase in proliferation (Fig. 5A), migration (Fig. 5B), invasion (Fig. 5C), and cell cycle progression (Fig. 5D) in both cell types. Furthermore, silencing of CCDC6 expression promoted proliferation (Fig. 5A), migration (Fig. 5B), invasion (Fig. 5C), and cell cycle progression (Fig. 5D) in both cell lines. These results suggest that CCDC6 is a functionally relevant target of miR-146b-5p in TPC-1 and BCPAP cell lines.

3.7. Inhibition of miR-146b-5p expression suppresses the proliferation of TPC-1 cells in vivo via upregulation of CCDC6 expression

To investigate the effect of miR-146b-5p expression on tumour growth and its interaction with CCDC6 *in vivo*, a stable CCDC6 overexpression TPC-1 cell line (Lenti-pGV367-CCDC6), a stable miR-146b-5p inhibition TPC-1 cell line (Lenti-pGV280-miR-146b-5p inhibitor), and the corresponding control cells were established and then injected into four groups of female BALB/c-nude mice (3.0×10^6 cells/mouse).

As shown in Fig. 6A, the xenografts derived from Lenti-miR-146b-5p-inhibitor and Lenti-pGV367-CCDC6 groups exhibited slower growth patterns than those derived from the control groups. At the end of the experiments, the weights of the tumours harvested from Lenti-pGV367-CCDC6 group (363.1 ± 31.97 mg) and Lenti-miR-146b-5p-inhibitor group (408.5 ± 10.71 mg) were significantly lower than weights of tumours harvested from the control groups (CCDC6 control group: 611.9 ± 9.29 mg, miR-146b-5p-inhibitor control group: 602.9 ± 11.92 mg) (Fig. 6B). Representative images are shown in Fig. 6C and D.

We examined the expression of CCDC6 in tumour xenograft using IHC and found a concurrent increase in CCDC6 expression in Lenti-miR-146b-5p-inhibitor tumour sections as compared with tumour sections from the control groups (Fig. 7A and B). Taken together, these results confirmed that the suppression of miR-146b-5p expression results in the inhibition of the tumour growth from TPC-1 cells *in vivo* via upregulation of CCDC6 expression.

3.8. CCDC6 expression is negatively correlated with the malignant characteristics of PTC

To assess the prognostic value of CCDC6, IHC was performed in 187 cases of PTC and the corresponding non-cancerous sections. The characteristics of study cases are listed in Table 2. The staining results revealed the lack of association between CCDC6 expression in PTC and age, gender, or tumour size. The low level of CCDC6 expression was closely related with malignant tissue ($p < 0.001$), lymph node metastasis ($p = 0.009$), extra-thyroid invasion ($p = 0.003$), and advanced TNM stages ($p = 0.044$).

Overall, these findings suggest the negative association between the expression of CCDC6 and the malignant phenotypes of PTC.

4. Discussion

Several recent studies have demonstrated the dysregulated expression of miRNAs in PTCs as well as the functions of miRNAs as oncogenes or tumour suppressors [17]. The expression of miR-146b-5p has been reported in almost all human organs and is thought to be involved in the pathogenesis of various human diseases such as atherosclerosis [18] and early allograft dysfunction post-liver transplantation [19]. Aberrant expression of miR-146b-5p is implicated in a variety of cancers, including renal [20], gastric [21], neuroblastoma [22], colorectal [23] and non-small cell lung [24] cancers.

The role of miR-146b-5p as an oncomiR was first identified in a study by Geraldo et al., wherein the overexpression of miR-146b-5p was associated with the aggressiveness of PTC [25]. In lung cancer, Patnaik et al. showed that the high expression level of miR-146b was predictive of recurrence [26]. Zhu et al. found that miR-146–5p was an oncogenic miRNA in colorectal cancer [23]. However, there are conflicting reports that support the role of miR-146b-5p as a tumour suppressor. miR-146b-5p was thought to function as a suppressor miRNA and its expression correlated with the prognosis of non-small cell lung cancer [24]. These contrasting roles of miR-146b-5p may be associated with the different targets repressed by this miRNA in different tissues as well as the regulation of its functions via a complex network in a tissue- and stage-dependent manner. The precise molecular mechanisms underlying miR-146b-5p-mediated regulation of PTC development are still unknown.

Based on a cohort of 92 PTC specimens, we demonstrated the positive correlation between miR-146b-5p expression and lymph node metastasis, extra-thyroidal invasion, and advanced clinical TNM stage

in PTC. We also confirmed that the suppression of miR-146b-5p expression resulted in the inhibition of TPC-1 and BCPAP cell proliferation, migration and invasion as well as cell cycle progression, while restoration of miR-146b-5p expression reversed the malignant characteristics.

In thyroid cancer, miR-146b-5p prompted the development and metastasis of PTC via targeting zinc and ring finger 3 (ZNRF3) [27] and mothers against decapentaplegic homolog 4 (SMAD4) [28]. In this study, we demonstrated that CCDC6 was involved in the development of PTC by acting as a functional target of miR-146b-5p, as evident from the following observations: (1) restoration of miR-146b-5p expression markedly diminished CCDC6 expression *in vitro*; (2) reintroduction of miR-146b-5p decreased the activity of luciferase reporter plasmids WT1 and WT2 but not that of MUT1 or MUT2 plasmid; (3) the upregulated miR-146b-5p expression promoted PTC development *in vitro* and *in vivo* with a concurrent reduction in CCDC6 expression; (4) restoration of CCDC6 expression attenuated the oncogenic characteristics.

CCDC proteins exhibit a highly versatile folding motif and are involved in multiple cellular biological processes in various neoplasms, such as CCDC116 in pancreatic cancer [29], CCDC62 in prostate cancer [30], CCDC98 in breast cancer [31], and CCDC134 in gastric cancer [32], via genetic or epigenetic alterations [33,34].

We assessed the function of CCDC6 in PTC *in vitro* and *in vivo*. IHC staining showed negative or weak staining results of CCDC6 in PTC sections, while intense staining bands were observed in the corresponding normal sections. We found that the expression of CCDC6 negatively correlated with cervical lymph node metastasis, extra-thyroidal invasion, and advanced clinical TNM stages. For the first time, our results supported the role of CCDC6 as a tumour suppressor in PTC and demonstrated the negative correlation between CCDC6 expression and malignant phenotypes of PTC.

In contrast to the results of the present study, Leone et al. [35] revealed the tumour-promoting role of CCDC6 in PTC harbouring the RET/PTC1 oncogene. The conflicting findings may be attributed to sampling variation and different manipulations of *CCDC6* gene.

Although our results indicated that the ectopic expression of miR-146b-5p induced the malignant phenotype of PTC via CCDC6 targeting, the signalling pathway of the miR-146b-5p/CCDC6 axis remains to be clarified.

The expression of miR-146b-5p induces epithelial-mesenchymal transition (EMT) by targeting zinc finger E-box-binding homeobox 1 (ZEB-1) and protein kinase B (Akt) in osteosarcoma [36] or by targeting ZRF-3 and enhancing Wnt/β-catenin signalling pathway expression in thyroid cancer [27]. Geraldo et al. showed that miR-146b-5p may disrupt the transferrin growth factor (TGF)-β signalling pathway and contribute to tumourigenesis in PTC [28]. During TGF-β-induced EMT, miR-146b-5p expression was upregulated with an increase in cancer stemness in PTC cells [37]. These data suggest the active role of miR-146b-5p in a complicated network of signalling pathways, including phosphatidylinositol-4,5-bisphosphate 3-kinase (PI3K)/Akt, TGF-β, Wnt/β-catenin and EMT, which warrants a more comprehensive investigation.

Taken together, this study highlights the functional role of miR-146b-5p as an oncomiR in PTC *in vitro* and *in vivo*. The function of miR-146b-5p is partly mediated through its direct binding to the 3′-UTR of CCDC6, which is proven as a tumour suppressor gene in PTC *in vitro* and *in vivo*. We also demonstrate that both miR-146b-5p and CCDC6 expression correlated with clinicopathological parameters and exerts significant diagnostic and prognostic values in patients with PTC. miR-146b-5p may be used as a novel therapeutic target of PTC treatment; further studies are warranted to investigate the related molecular signalling pathway.

Conflicts of interest

The above authors declare NO conflict of interest.

Acknowledgements

The authors would like to acknowledge the experimental assistance from Prof. Yi Zhang and Dr. Qianyi He (Biotherapy Center, The First Affiliated Hospital of Zhengzhou University). We are also grateful to Prof. Lili Zheng (Department of Endocrinology, The First Affiliated Hospital of Zhengzhou University) for providing the TPC-1 cell line and Dr. Shuiying Zhao (Department of Endocrinology, The First Affiliated Hospital of Zhengzhou University) for providing the BCPAP and NTHY cell lines. This work was supported by the Key Scientific and Technological Project, Department of Technology, Henan Province, China (172102310390) and the Key Scientific and Technological Project, Department of Education, Henan Province, China (17A320030).

Appendix A. Supplementary data

Supplementary data to this article can be found online at https://doi.org/10.1016/j.canlet.2018.11.026.

References

[1] C.K. Jung, M.P. Little, J.H. Lubin, A.V. Brenner, S.A. Wells Jr., A.J. Sigurdson, Y.E. Nikiforov, The increase in thyroid cancer incidence during the last four decades is accompanied by a high frequency of BRAF mutations and a sharp increase in RAS mutations, J. Clin. Endocrinol. Metab. 99 (2014) E276–E285.
[2] N. Cancer Genome Atlas Research, Integrated genomic characterization of papillary thyroid carcinoma, Cell 159 (2014) 676–690.
[3] J. Jendrzejewski, A. Thomas, S. Liyanarachchi, A. Eiterman, J. Tomsic, H. He, H.S. Radomska, W. Li, R. Nagy, K. Sworczak, A. de la Chapelle, PTCSC3 is involved in papillary thyroid carcinoma development by modulating S100A4 gene expression, J. Clin. Endocrinol. Metab. 100 (2015) E1370–E1377.
[4] K.L. Kojic, S.L. Kojic, S.M. Wiseman, Differentiated thyroid cancers: a comprehensive review of novel targeted therapies, Expet Rev. Anticancer Ther. 12 (2012) 345–357.
[5] B.J. Hale, C.X. Yang, J.W. Ross, Small RNA regulation of reproductive function, Mol. Reprod. Dev. 81 (2014) 148–159.
[6] A. Ventura, T. Jacks, MicroRNAs and cancer: short RNAs go a long way, Cell 136 (2009) 586–591.
[7] E. Minna, P. Romeo, L. De Cecco, M. Dugo, G. Cassinelli, S. Pilotti, D. Degl'Innocenti, C. Lanzi, P. Casalini, M.A. Pierotti, A. Greco, M.G. Borrello, miR-199a-3p displays tumor suppressor functions in papillary thyroid carcinoma, Oncotarget 5 (2014) 2513–2528.
[8] W. Qiu, Z. Yang, Y. Fan, Q. Zheng, MicroRNA-613 inhibits cell growth, migration and invasion of papillary thyroid carcinoma by regulating SphK2, Oncotarget 7 (2016) 39907–39915.
[9] A. Wojcicka, M. Kolanowska, K. Jazdzewski, Mechanisms in endocrinology: MicroRNA in diagnostics and therapy of thyroid cancer, Eur. J. Endocrinol./ European Federation of Endocrine Societies 174 (2016) R89–R98.
[10] J. Zhang, Y. Liu, Z. Liu, X.M. Wang, D.T. Yin, L.L. Zheng, D.Y. Zhang, X.B. Lu, Differential expression profiling and functional analysis of microRNAs through stage I-III papillary thyroid carcinoma, Int. J. Med. Sci. 10 (2013) 585–592.
[11] A. Celetti, A. Cerrato, F. Merolla, D. Vitagliano, G. Vecchio, M. Grieco, H4(D10S170), a gene frequently rearranged with RET in papillary thyroid carcinomas: functional characterization, Oncogene 23 (2004) 109–121.
[12] M. Grieco, M. Santoro, M.T. Berlingieri, R.M. Melillo, R. Donghi, I. Bongarzone, M.A. Pierotti, G. Della Porta, A. Fusco, G. Vecchio, PTC is a novel rearranged form of the ret proto-oncogene and is frequently detected in vivo in human thyroid papillary carcinomas, Cell 60 (1990) 557–563.
[13] K. Takeuchi, M. Soda, Y. Togashi, R. Suzuki, S. Sakata, S. Hatano, R. Asaka, W. Hamanaka, H. Ninomiya, H. Uehara, Y. Lim Choi, Y. Satoh, S. Okumura, K. Nakagawa, H. Mano, Y. Ishikawa, RET, ROS1 and ALK fusions in lung cancer, Nat. Med. 18 (2012) 378–381.
[14] F. Merolla, F. Pentimalli, R. Pacelli, G. Vecchio, A. Fusco, M. Grieco, A. Celetti, Involvement of H4(D10S170) protein in ATM-dependent response to DNA damage, Oncogene 26 (2007) 6167–6175.
[15] V. Leone, C. Langella, F. Esposito, M. De Martino, M. Decaussin-Petrucci, G. Chiappetta, A. Bianco, A. Fusco, miR-130b-3p upregulation contributes to the development of thyroid adenomas targeting CCDC6 gene, Eur Thyroid J 4 (2015) 213–221.
[16] C. Wittekind, I. Tischoff, [Tumor classifications], Pathologe 25 (2004) 481–490.
[17] M. Celano, MicroRNAs as Biomarkers in Thyroid Carcinoma, (2017), p. 2017.
[18] N. Lin, Y. An, Blockade of 146b-5p promotes inflammation in atherosclerosis-associated foam cell formation by targeting TRAF6, Experimental and therapeutic medicine 14 (2017) 5087–5092.
[19] C. Li, Q. Zhao, W. Zhang, M. Chen, W. Ju, L. Wu, M. Han, Y. Ma, X. Zhu, D. Wang, Z. Guo, X. He, MicroRNA-146b-5p identified in porcine liver donation model is associated with early allograft dysfunction in human liver transplantation, Med. Sci. Mon. Int. Med. J. Exp. Clin. Res. : Int. Med. J. Exp. Clin. Res. 23 (2017) 5876–5884.

[20] F.Q. Yang, J.Q. Zhang, J.J. Jin, C.Y. Yang, W.J. Zhang, H.M. Zhang, J.H. Zheng, Z.M. Weng, HOXA11-AS promotes the growth and invasion of renal cancer by sponging miR-146b-5p to upregulate MMP16 expression, J. Cell. Physiol. 233 (2018) 9611–9619.
[21] W. Wang, M. Du, Z. Li, L. Zhang, Q. Li, Z. Xu, B. Li, L. Wang, F. Li, D. Zhang, H. Xu, L. Yang, W. Gong, F. Qiang, Z. Zhang, Z. Xu, A genetic variant located in miR-146b promoter region is associated with prognosis of gastric cancer, cancer epidemiology, biomarkers & prevention : a publication of the american association for cancer research, Cosponsored by the American Society of Preventive Oncology 27 (2018) 822–828.
[22] T. Xu, H.Q. Xie, Y. Li, Y. Xia, R. Sha, L. Wang, Y. Chen, L. Xu, B. Zhao, Dioxin induces expression of hsa-miR-146b-5p in human neuroblastoma cells, J. Environ. Sci. (China) 63 (2018) 260–267.
[23] Y. Zhu, G. Wu, W. Yan, H. Zhan, P. Sun, miR-146b-5p regulates cell growth, invasion, and metabolism by targeting PDHB in colorectal cancer, American journal of cancer research 7 (2017) 1136–1150.
[24] Y. Li, H. Zhang, Y. Dong, Y. Fan, Y. Li, C. Zhao, C. Wang, J. Liu, X. Li, M. Dong, H. Liu, J. Chen, MiR-146b-5p functions as a suppressor miRNA and prognosis predictor in non-small cell lung cancer, J. Canc. 8 (2017) 1704–1716.
[25] M.V. Geraldo, C.S. Fuziwara, C.U. Friguglieti, R.B. Costa, M.A. Kulcsar, A.S. Yamashita, E.T. Kimura, MicroRNAs miR-146-5p and let-7f as prognostic tools for aggressive papillary thyroid carcinoma: a case report, Arquivos Brasileiros Endocrinol. Metabol. 56 (2012) 552–557.
[26] S.K. Patnaik, E. Kannisto, R. Mallick, S. Yendamuri, Overexpression of the lung cancer-prognostic miR-146b microRNAs has a minimal and negative effect on the malignant phenotype of A549 lung cancer cells, PloS One 6 (2011) e22379.
[27] X. Deng, B. Wu, K. Xiao, J. Kang, J. Xie, X. Zhang, Y. Fan, MiR-146b-5p promotes metastasis and induces epithelial-mesenchymal transition in thyroid cancer by targeting ZNRF3, Cellular physiology and biochemistry, international journal of experimental cellular physiology, biochemistry, and pharmacology 35 (2015) 71–82.
[28] M.V. Geraldo, A.S. Yamashita, E.T. Kimura, MicroRNA miR-146b-5p regulates signal transduction of TGF-beta by repressing SMAD4 in thyroid cancer, Oncogene 31 (2012) 1910–1922.
[29] A.V. Tsolakis, L. Grimelius, M.S. Islam, Expression of the coiled coil domain containing protein 116 in the pancreatic islets and endocrine pancreatic tumors, Islets 4 (2012) 349–353.
[30] M. Chen, J. Ni, H.C. Chang, C.Y. Lin, M. Muyan, S. Yeh, CCDC62/ERAP75 functions as a coactivator to enhance estrogen receptor beta-mediated transactivation and target gene expression in prostate cancer cells, Carcinogenesis 30 (2009) 841–850.
[31] D.J. Novak, N. Sabbaghian, P. Maillet, P.O. Chappuis, W.D. Foulkes, M. Tischkowitz, Analysis of the genes coding for the BRCA1-interacting proteins, RAP80 and Abraxas (CCDC98), in high-risk, non-BRCA1/2, multiethnic breast cancer cases, Breast Canc. Res. Treat. 117 (2009) 453–459.
[32] J. Zhong, M. Zhao, Q. Luo, Y. Ma, J. Liu, J. Wang, M. Yang, X. Yuan, J. Sang, C. Huang, CCDC134 is down-regulated in gastric cancer and its silencing promotes cell migration and invasion of GES-1 and AGS cells via the MAPK pathway, Mol. Cell. Biochem. 372 (2013) 1–8.
[33] P. Burkhard, J. Stetefeld, S.V. Strelkov, Coiled coils: a highly versatile protein folding motif, Trends Cell Biol. 11 (2001) 82–88.
[34] B. Kokona, Z.P. Rosenthal, R. Fairman, Role of the coiled-coil structural motif in polyglutamine aggregation, Biochemistry 53 (2014) 6738–6746.
[35] V. Leone, C. Langella, F. Esposito, C. Arra, G. Palma, D. Rea, O. Paciello, F. Merolla, D. De Biase, S. Papparella, A. Celetti, A. Fusco, Ccdc6 knock-in mice develop thyroid hyperplasia associated to an enhanced CREB1 activity, Oncotarget 6 (2015) 15628–15638.
[36] H.H. Al-Khalaf, A. Aboussekhra, MicroRNA-141 and microRNA-146b-5p inhibit the prometastatic mesenchymal characteristics through the RNA-binding protein AUF1 targeting the transcription factor ZEB1 and the protein kinase AKT, J. Biol. Chem. 289 (2014) 31433–31447.
[37] H. Hardin, Z. Guo, W. Shan, C. Montemayor-Garcia, S. Asioli, X.M. Yu, A.D. Harrison, H. Chen, R.V. Lloyd, The roles of the epithelial-mesenchymal transition marker PRRX1 and miR-146b-5p in papillary thyroid carcinoma progression, Am. J. Pathol. 184 (2014) 2342–2354.